crystals

MDPI

Article

Towards the Development of novel Diclofenac Multicomponent Pharmaceutical Solids

Francisco Javier Acebedo-Martínez [1], Carolina Alarcón-Payer [2], Helena María Barrales-Ruíz [1,3], Juan Niclós-Gutiérrez [3], Alicia Domínguez-Martín [3] and Duane Choquesillo-Lazarte [1,*]

Figure S1. PXRD patterns of the LAG screening experiments with the coformers of Table 2.

Figure S2. PXRD patterns of DIC—ADE, DIC—CYT and DIC—ICT after neat grinding.

Figure S3. PXRD patterns of DIC—ADE, DIC—CYT and DIC—ICT after LAG in methanol using different stoichiometries.

Figure S4. Experimental PXRD pattern of DIC—ADE, DIC—CYT and DIC—ICT, compared with DIC, coformers and the corresponding calculated powder patterns.

Figure S5. TGA traces of DIC–ADE (top), DIC—CYT (middle) and DIC–ICT (bottom).

Figure S6. PXRD patterns of DIC–ADE (top), DIC—CYT (middle) and DIC–ICT (bottom) with respect to the stability under accelerated ageing conditions (40 °C, 75% RH) at different time intervals.

Figure S7. PXRD patterns of DIC–ADE (top), DIC—CYT (middle) and DIC–ICT (bottom) after the stability slurry assay (at 25 ºC, during 24 h, in water).

Figure S8. Overlapping UV spectra of diclofenac (DIC) and nucleobase coformers (ADE: adenine, CYT: cytosine, ICT: isocytosine).

Figure S9. ORTEP representation showing the asymmetric unit of DIC—ADE with atom numbering scheme (thermal ellipsoids are plotted with the 50% probability level).

Figure S10. ORTEP representation showing the asymmetric unit of DIC—CYT with atom numbering scheme (thermal ellipsoids are plotted with the 50% probability level).

Figure S11. ORTEP representation showing the asymmetric unit of DIC—ICT with atom numbering scheme (thermal ellipsoids are plotted with the 50% probability level).

Table S1. Results of the LAG experiments between DIC and selected coformers.

Table S2. Hydrogen bonds for DIC—ADE [Å and deg.].

Table S3. Hydrogen bonds for DIC—CYT [Å and deg.].

Table S4. Hydrogen bonds for DIC—ICT [Å and deg.].

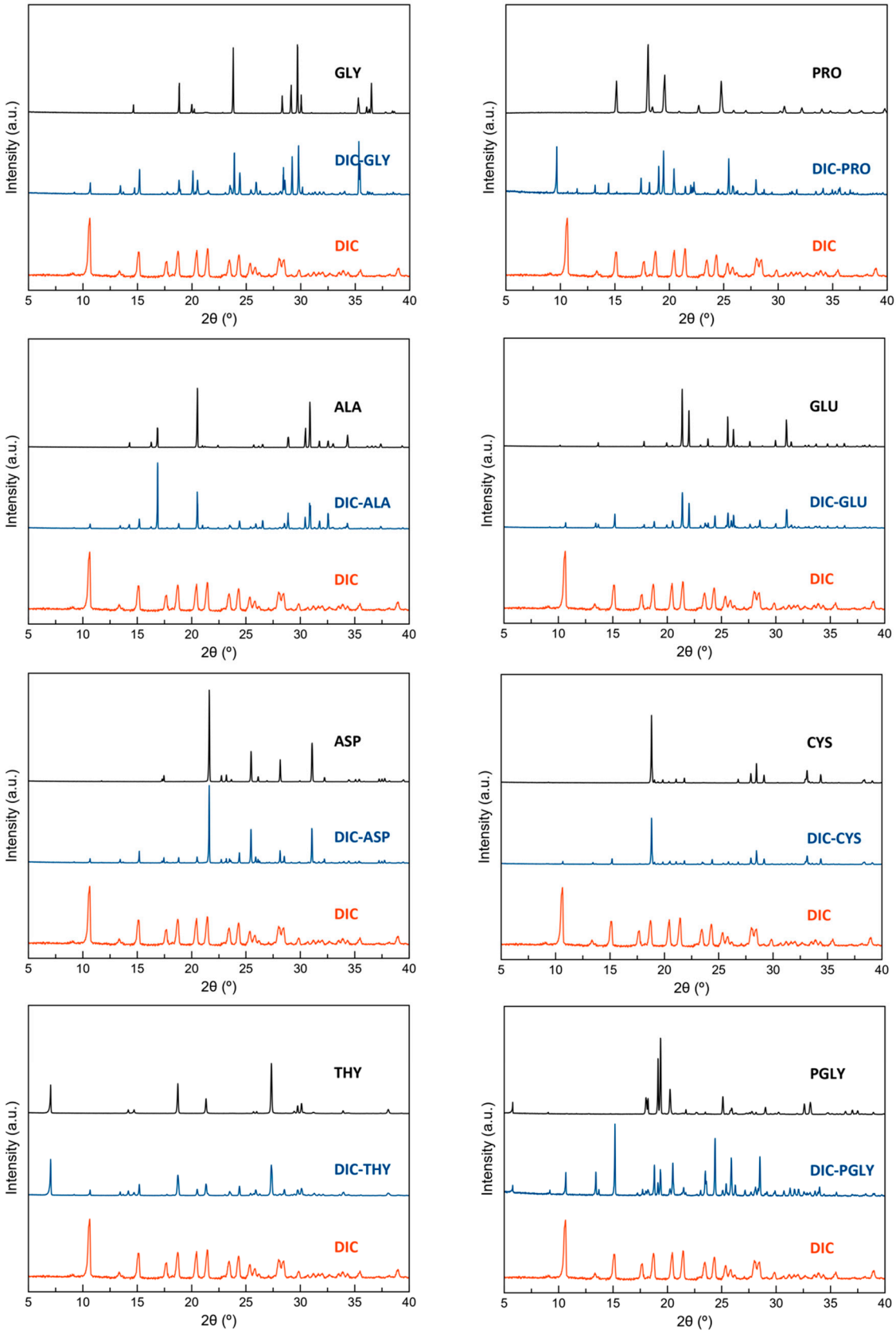

Figure S1. PXRD patterns of the LAG screening experiments with the coformers of Table 2. GLY: glycine; PRO: proline; ALA: alanine; GLU: glutamic acid; ASP: aspartic acid; CYS: cysteine; THY: thymine; PGLY: phenylglycine.

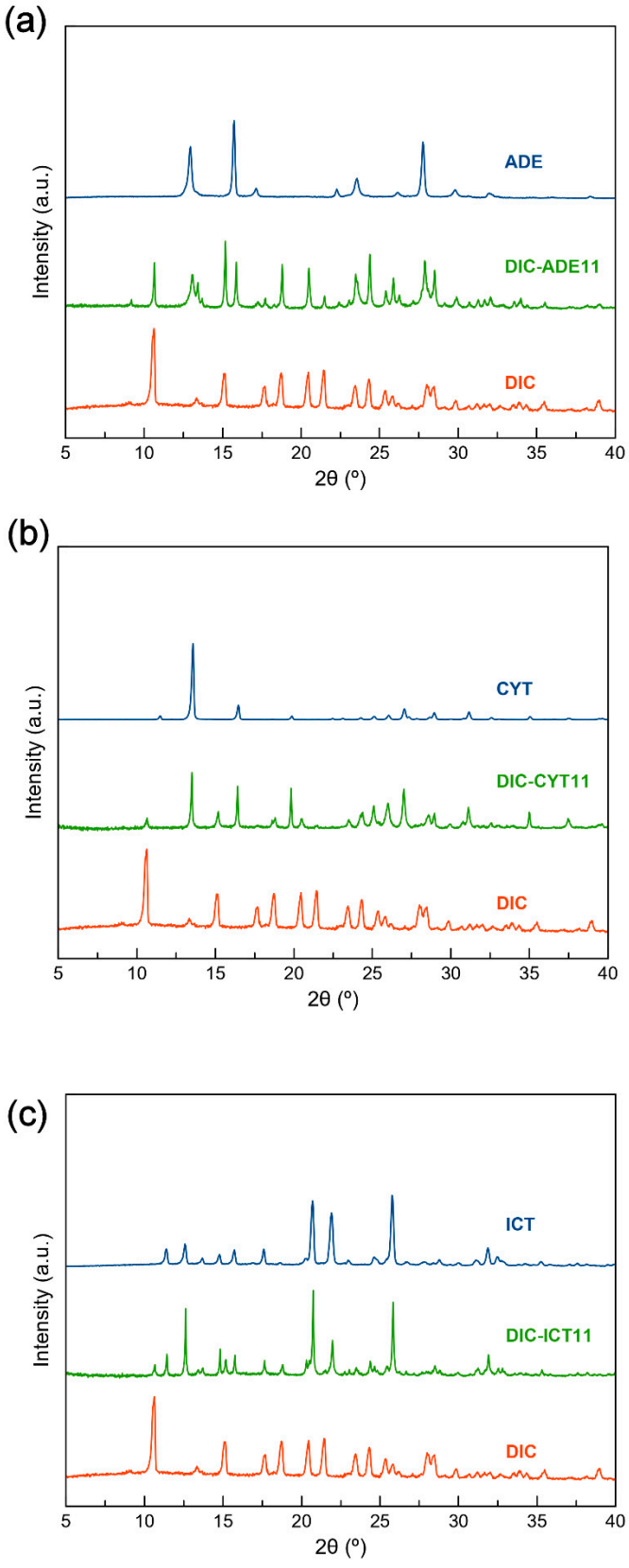

Figure S2. PXRD patterns of (a) DIC—ADE, (b) DIC—CYT and (c) DIC—ICT after neat grinding.

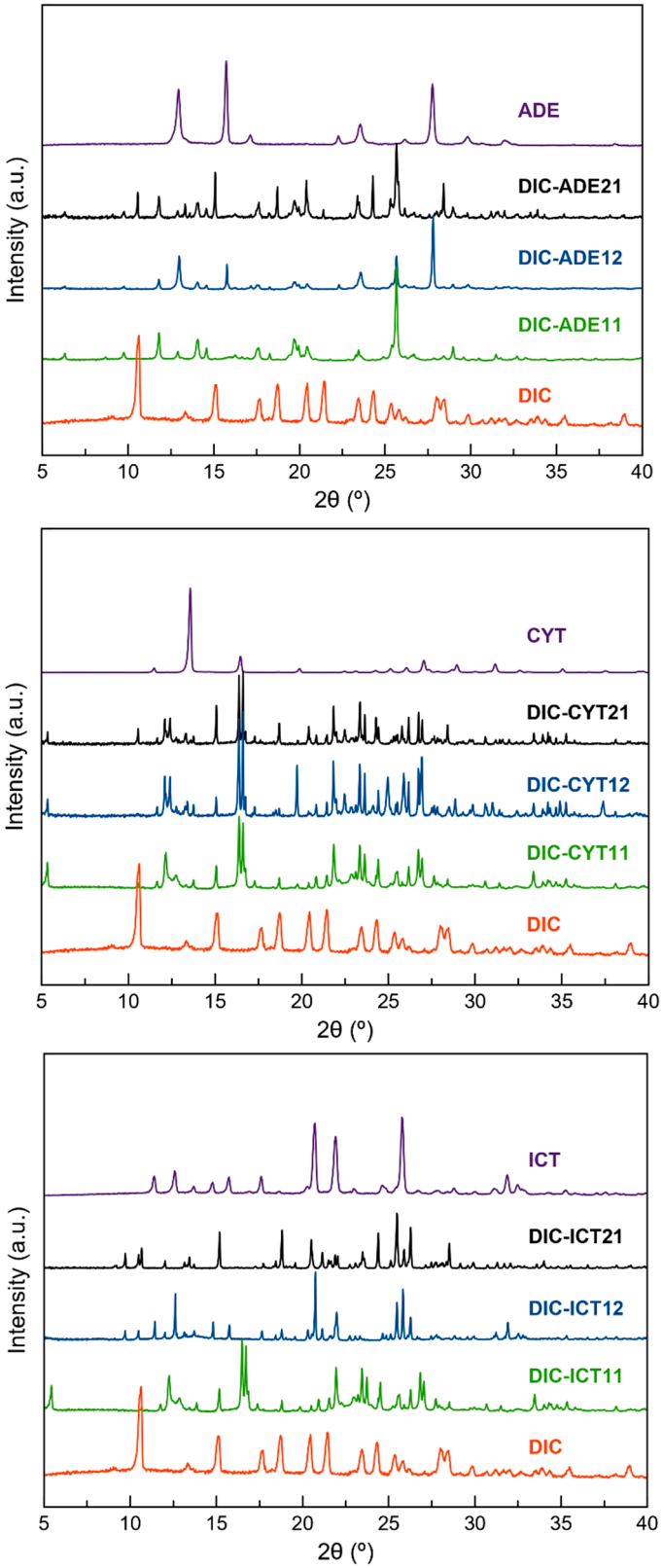

Figure S3. PXRD patterns of DIC—ADE (top), DIC—CYT (middle) and DIC—ICT (bottom) after LAG in methanol using different stoichiometries.

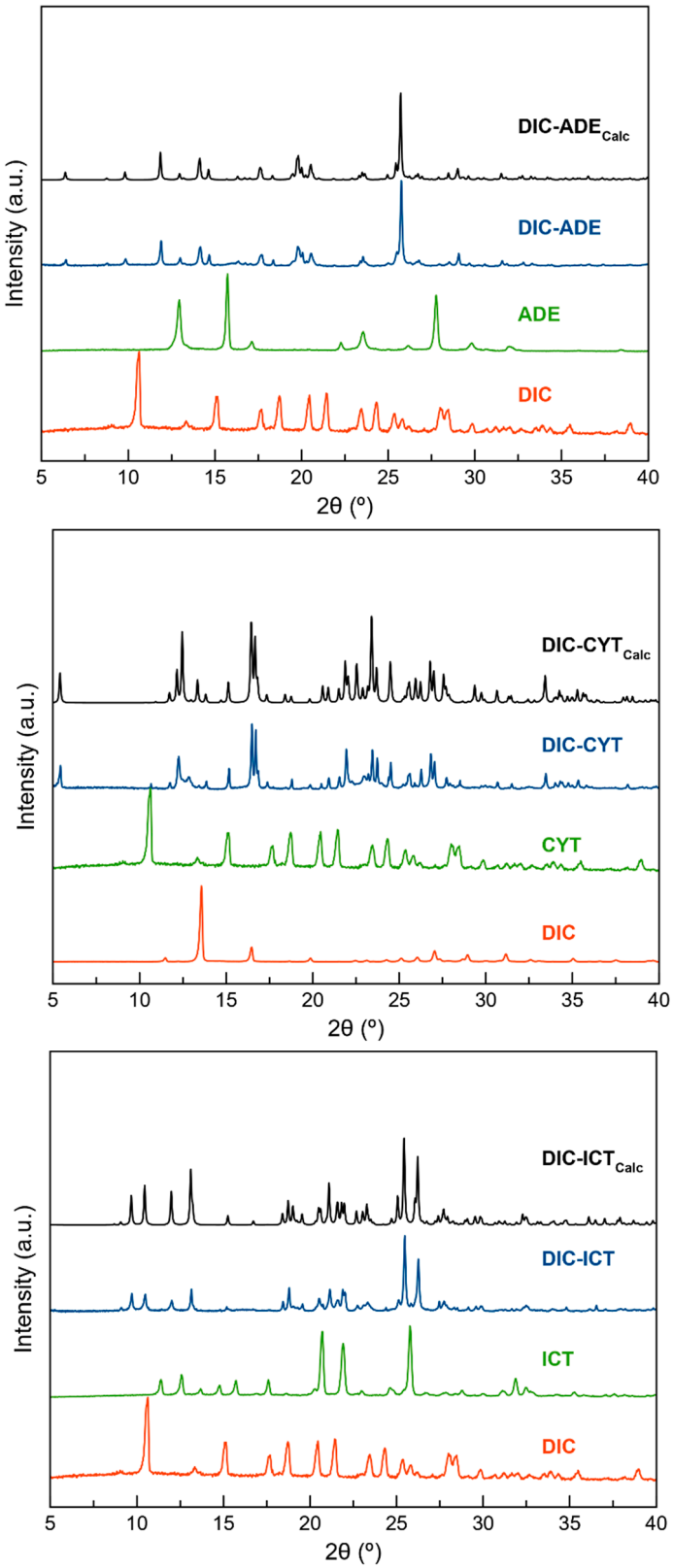

Figure S4. Experimental PXRD pattern of DIC—ADE (top), DIC—CYT (middle) and DIC—ICT (bottom), compared with DIC, coformers and the corresponding calculated powder patterns.

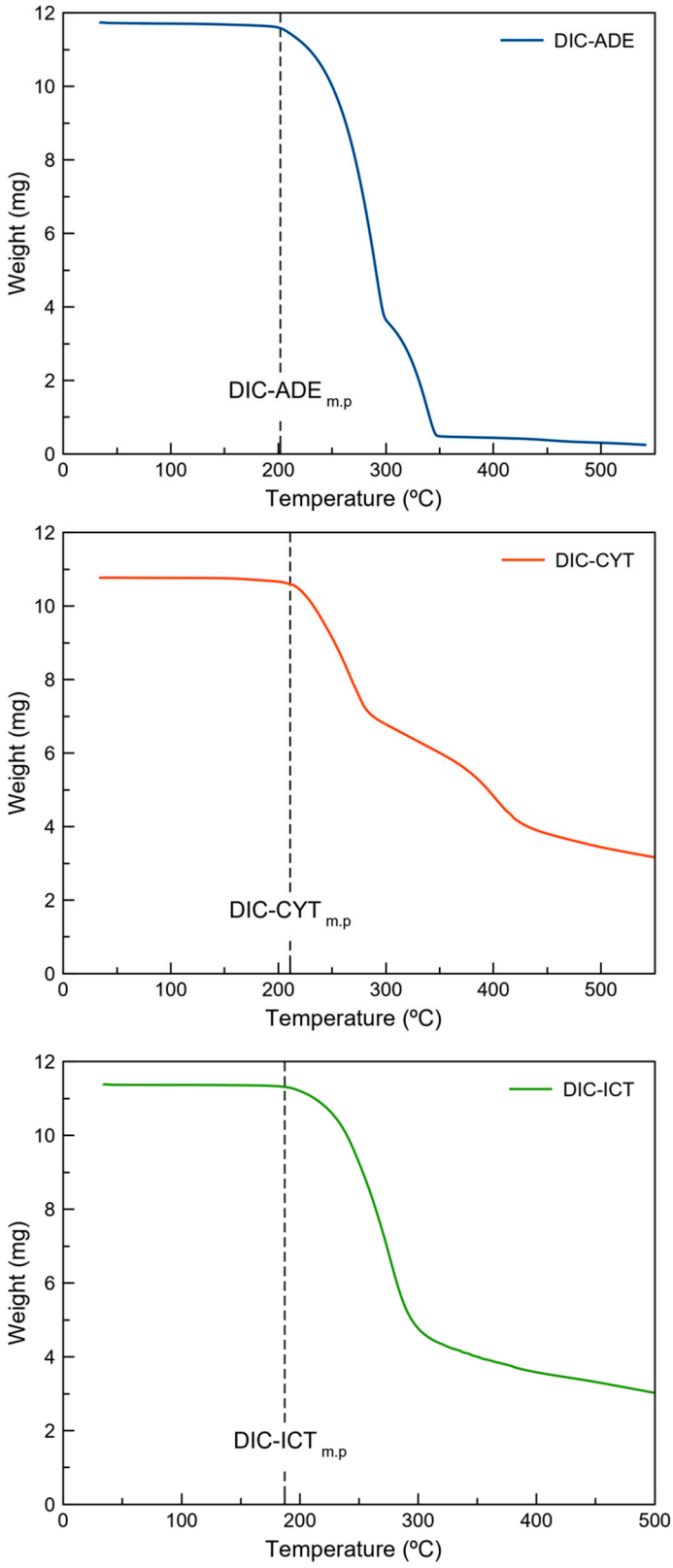

Figure S5. TGA traces of DIC–ADE (top), DIC—CYT (middle) and DIC–ICT (bottom).

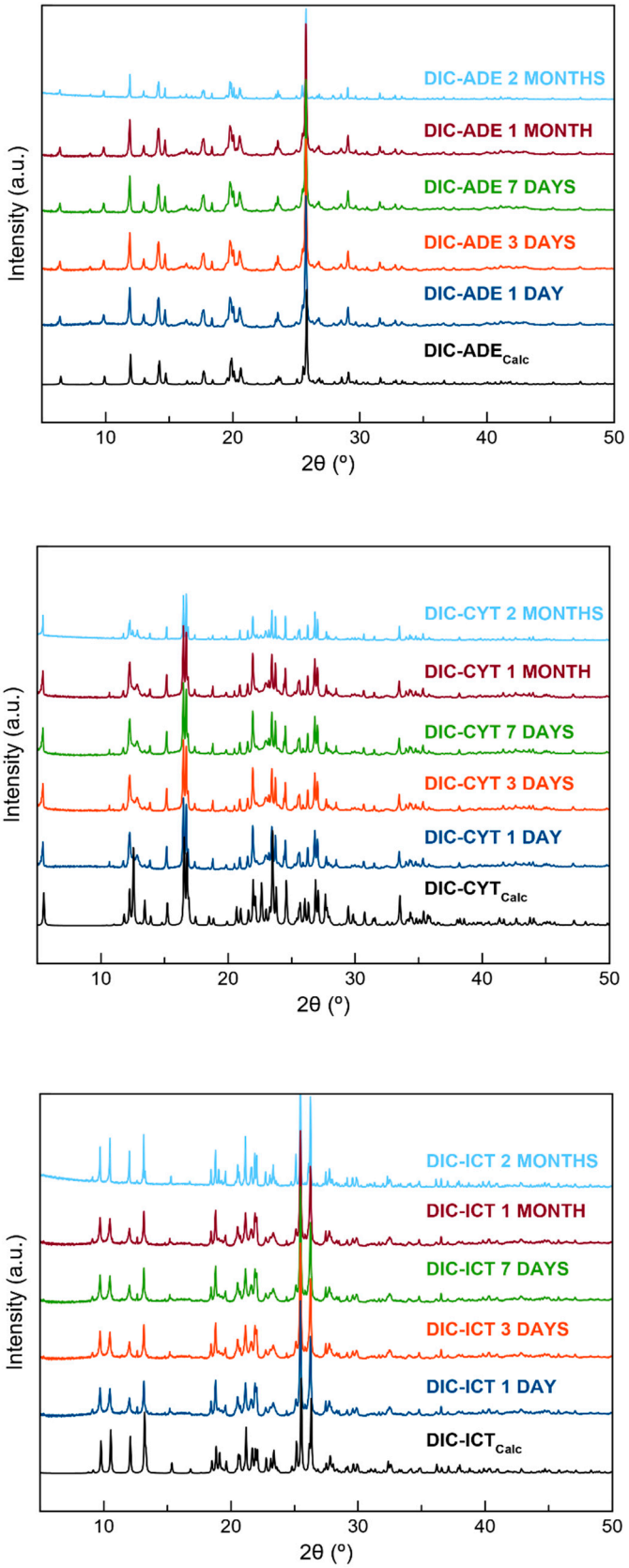

Figure S6. PXRD patterns of DIC–ADE (top), DIC—CYT (middle) and DIC–ICT (bottom) with respect to the stability under accelerated ageing conditions (40 °C, 75% RH) at different time intervals.

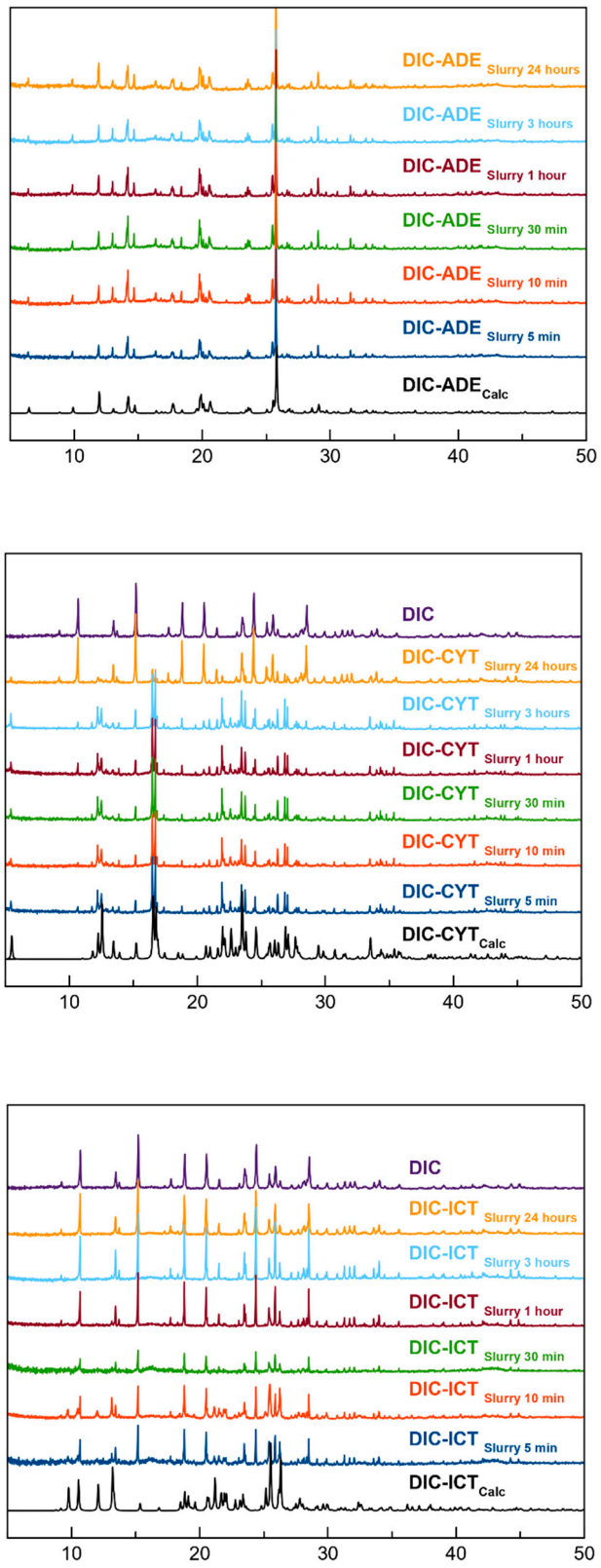

Figure S7. PXRD patterns of DIC–ADE (top), DIC—CYT (middle) and DIC–ICT (bottom) after the stability slurry assay (at 25 ºC, during 24 h, in water).

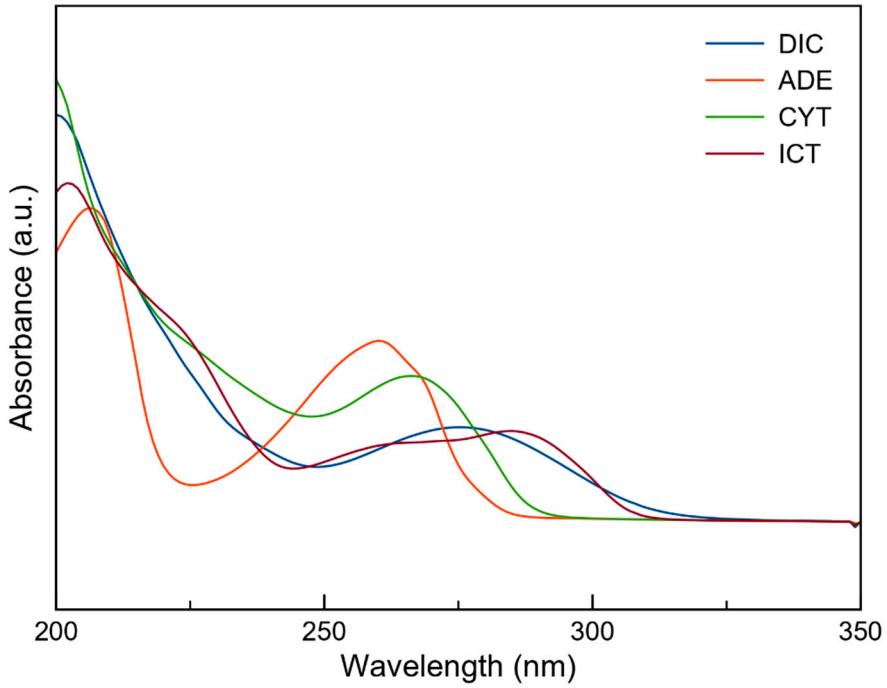

Figure S8. Overlapping UV spectra of diclofenac (DIC) and nucleobase coformers (ADE: adenine, CYT: cytosine, ICT: isocytosine).

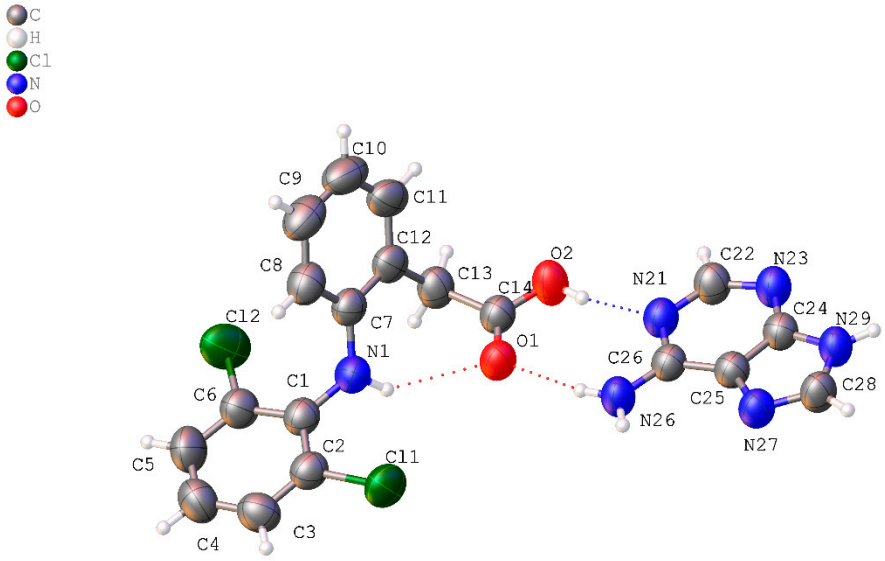

Figure S9. ORTEP representation showing the asymmetric unit of DIC—ADE with atom numbering scheme (thermal ellipsoids are plotted with the 50% probability level).

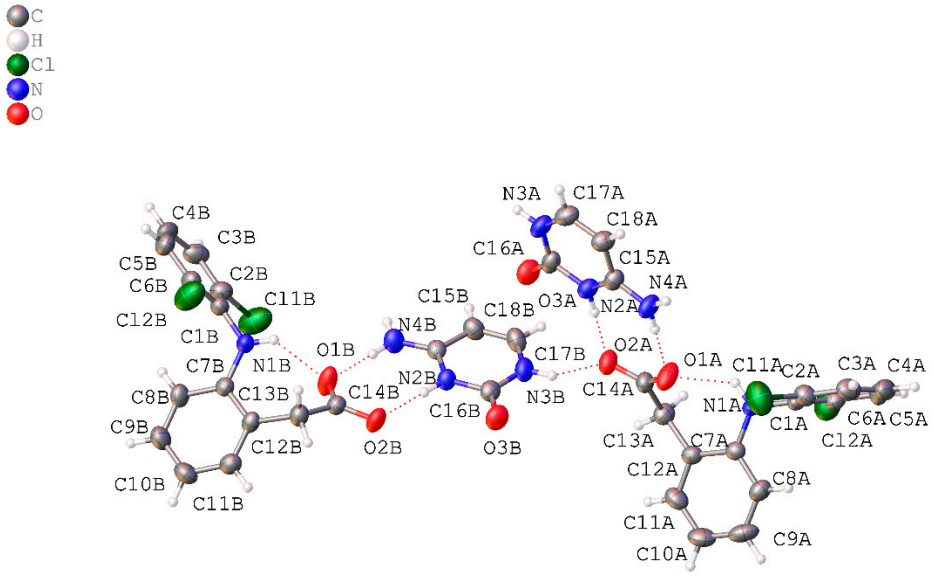

Figure S10. ORTEP representation showing the asymmetric unit of DIC—CYT with atom numbering scheme (thermal ellipsoids are plotted with the 50% probability level).

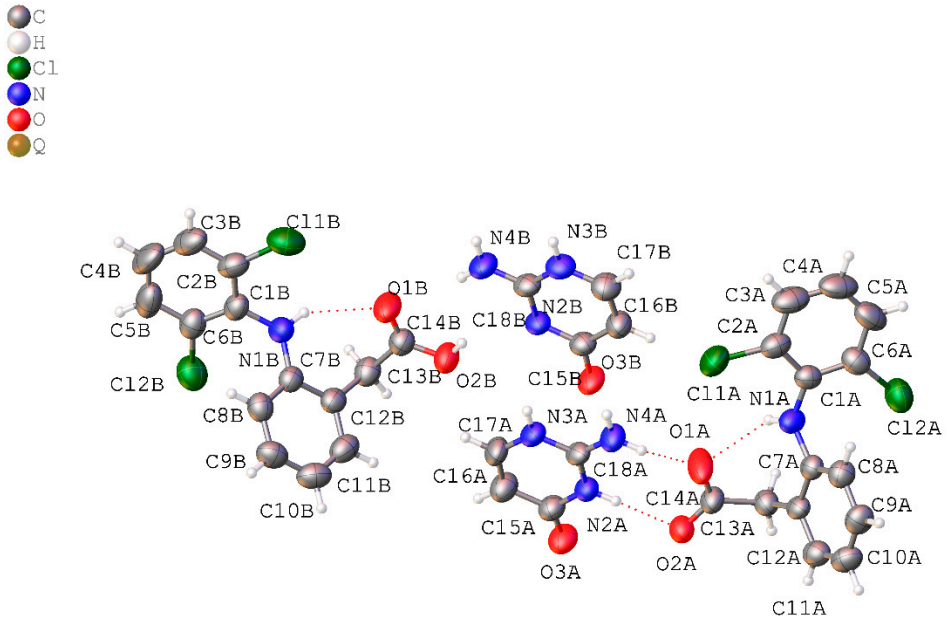

Figure S11. ORTEP representation showing the asymmetric unit of DIC—ICT with atom numbering scheme (thermal ellipsoids are plotted with the 50% probability level).

Table S1. Results of the LAG experiments between DIC and selected coformers.

Coformer	Solvent	Result
Glycine	MET, EOH, ACE	Physical mixture
Proline	EOH	Cocrystal reported [11]
Alanine	MET, EOH, ACE	Physical mixture
Glutamic Acid	MET, EOH, ACE	Physical mixture
Aspartic Acid	MET, EOH, ACE	Physical mixture
Cytosine	**MET**	**New phase, this work**
Adenine	**MET**	**New phase, this work**
Cysteine	MET, EOH, ACE	Physical mixture
Thymine	MET, EOH, ACE	Physical mixture
Phenylglycine	MET, EOH, ACE	Physical mixture
Isocytosine	**MET**	**New phase, this work**

Table S2. Hydrogen bonds for DIC—ADE [Å and deg.].

D-H···A	d(D-H)	d(H···A)	d(D···A)	<(DHA)
O(2)-H(2)···N(21)	0.82	1.84	2.650(2)	169.0
N(1)-H(1)···O(1)	0.86	2.38	3.005(2)	129.7
N(26)-H(26A) ···O(1)	0.86	2.10	2.946(3)	169.0
N(26)-H(26B)···N(27)#1	0.86	2.10	2.933(3)	162.5
N(29)-H(29)···N(23)#2	0.86	2.00	2.847(3)	166.6

Symmetry transformations used to generate equivalent atoms:

#1 -x+2,-y+1,-z #2 -x+3,-y+2,-z

Table S3. Hydrogen bonds for DIC—CYT [Å and deg.].

D-H···A	d(D-H)	d(H···A)	d(D···A)	<(DHA)
N(1A)-H(1A)···O(1A)	0.86	2.18	2.739(7)	122.1
N(1B)-H(1B)···O(1B)	0.86	2.17	2.737(6)	123.3
N(2A)-H(2A)···O(2A)	0.86	1.92	2.778(7)	176.3
N(3A)-H(3AA)···O(2B)#1	0.86	1.96	2.729(6)	148.9
N(4A)-H(4AA)···O(1A)	0.86	1.85	2.705(7)	178.0
N(4A)-H(4AB)···O(3A)#2	0.86	1.98	2.840(7)	179.1
N(2B)-H(2B)···O(2B)	0.86	1.92	2.780(6)	176.5
N(3B)-H(3BA)···O(2A)	0.86	1.94	2.727(6)	152.2
N(4B)-H(4BA)···O(1B)	0.86	1.84	2.699(7)	178.4
N(4B)-H(4BB)···O(3B)#3	0.86	1.99	2.851(7)	178.5

Symmetry transformations used to generate equivalent atoms:

#1 x,y-1,z #2 x-1/2,-y,z #3 x+1/2,-y+1,z

Table S4. Hydrogen bonds for DIC—ICT [Å and deg.].

D-H···A	d(D-H)	d(H···A)	d(D···A)	<(DHA)
N(1A)-H(1A)···O(1A)	0.86	2.26	2.846(9)	125.5
O(2B)-H(2B)···N(2B)#1	0.82	1.80	2.618(9)	171.7
N(1B)-H(1B)···O(1B)	0.86	2.41	3.000(10)	126.4
N(2A)-H(2A)···O(2A)	0.86	1.99	2.844(8)	174.0
N(3A)-H(3AA)···O(3B)#1	0.86	2.03	2.774(9)	144.5
N(4A)-H(4AA)···O(3B)#1	0.86	2.01	2.761(8)	146.0
N(4A)-H(4AB)···O(1A)	0.86	1.82	2.637(9)	158.1
N(3B)-H(3BA)···O(2A)#2	0.86	1.91	2.768(8)	178.7
N(4B)-H(4BA)···O(1B)#3	0.86	2.02	2.864(11)	166.4
N(4B)-H(4BB)···O(3A)#2	0.86	2.09	2.829(9)	144.2

Symmetry transformations used to generate equivalent atoms:

#1 x+1,y,z #2 x+1,y-1,z #3 x-1,y,z